

Temperature glide matching in a zeotropic mixture heat pump

V. Venzik^a and B. Atakan^b

^a *University of Duisburg-Essen, Thermodynamics, Duisburg, Germany, valerius.venzik@uni-due.de*

^b *University of Duisburg-Essen, Thermodynamics, Duisburg, Germany, burak.atakan@uni-due.de*

Abstract:

The use of zeotropic mixtures in heat pumps should lead to a reduction of the exergy losses within the heat exchangers due to the temperature glide (TG) and thus to an improvement of the entire process. In a previous publication (ECOS 2016), the coefficient of performance (COP) as a function of evaporation/condensation temperature, compressor rotation speed and composition of a zeotropic mixture (isobutane/propene) was investigated. Contrary to theoretical analysis, it was shown that the COPs of the mixtures increase only slightly compared to the better performing pure fluid. The temperature change of the secondary fluid in the heat exchangers was relatively small. In the present work, it is experimentally investigated whether a better matching of the temperature glide in the evaporator raises the COP of a zeotropic mixture compared to the better performing pure fluid. The targeted utilization of the TG is achieved by matching the temperature variation of the mixture and the temperature variation of the heat source; this was adjusted by varying the heat capacity flowrate of the source. An isobutane/propene mixture (42:58) with a TG of 8.03 K is investigated as the working fluid, together with investigations of the pure fluids isobutane and propene, all for equal boundary conditions. The experiments were carried out for a fix evaporator inlet temperature and two compressor rotation speeds. The exergy losses of individual components, and for the whole cycle, like exergetic efficiencies and COPs, were determined and were compared. In case of an optimal temperature match between the heat source and the refrigerant in the evaporator, contrary to the expectation, the COP of the mixture decreases by 4.2 % while the second law efficiency of the entire processes increases by 18.15 %.

Keywords:

Temperature glide matching, refrigerant mixture, vapour compression heat pump

1. Introduction

Presently, some well-established refrigerants from the substance group of HFCs (hydrofluorocarbons) like R134a, R404a, R407c and R410a are used in vapour compression based refrigeration cycles in air conditioning and in heat pump units. However, the regulation (No 517/2014) of the European Union [1] prohibits the use of HFCs with a GWP (Global Warming Potential) above 150 in commercial refrigeration devices, coolers and heat pumps from the year 2022. Therefore, it is essential to investigate alternative fluids for vapour compression systems with respect to ecological aspects (zero ozone depletion potential (ODP) and low GWP) besides the general criteria like thermal efficiency and costs. Alkanes represent an appropriate fluid group with good thermodynamic properties and good material compatibility; they are miscible with commonly applied lubricants, easily available, cost-efficient and environmentally friendly. Pure fluids like propane and isobutane are already used in many European refrigerators. Apart from pure fluids, the use of zeotropic mixtures in vapor compression systems is widely discussed (see e.g. [2], [3]). From the theoretical point of view; simple thermodynamic calculations with a constant compressor isentropic efficiency and similar operating conditions show a high potential to improve the COP by 30 % using a zeotropic mixture of isobutene/propene in comparison to propene as an example. The advantage of a zeotropic mixture, in comparison to a pure fluid, is based on the non-isothermal phase change, known as the temperature glide (TG), which offers the possibility to reduce the mean temperature difference between the refrigerant and the secondary fluid in the heat exchanger. This leads in turn to a reduced difference between the thermodynamic mean temperatures of the heat

source and refrigerant, and thus, to an improved performance of the entire process with respect to the energetic and exergetic efficiencies. Based on this theoretical approach, several scientists investigated pure HCs (hydrocarbons) and their mixtures, to find an adequate fluid in order to replace CFCs and HFCs. Chang et. al. [4] investigated experimentally the performances and the heat transfer characteristics of four pure fluids (isobutane (R600a), butane (R600), propane (R290) and propene (R1270)) and furthermore of two mixtures composed of R290, R600a and R600 in order to replace R22 in a heat pump. Their results indicate that the COP of the binary mixture R290/R600a (in a ratio of 50:50 by mass) and R290/R600 (in a ratio of 75:25 by mass) increases by 7 and 11 % in comparison to R22, respectively. However, the COP for the best mixture is, compared to the better pure fluid (propane), only slightly better. Park and Jung [5] carried out a further experimental investigation, aiming to replace R22 by a mixture. In their work, the performance of a heat pump charged with R170/R290 was studied for five different mass fractions of R170 (between 2 and 10 %). It is shown that the cooling and heating rates increase with increasing mass fraction of ethane while the COP of the mixture decreases continuously. Compared to R22, the mixture with a mass fraction of 4 % ethane achieved a similar COP as well as similar cooling/heating rates and is therefore identified as a long-term alternative for R22. Aiming to find an R22 replacement for residential air conditioning applications, Park et. al. [6] investigated the thermodynamic performance of two pure fluids (R290 and R1270) and seven mixtures composed of R1270, R290, R152a and dimethyl ether (RE170) experimentally. Here, the best COP was reached by the ternary mixture composed of 45:40:15 by mass of R1270/290/RE170. However, in comparison to the best performing pure fluid, propane, the ternary mixture enhanced the COP only by 3.5 %. Richardson and Butterworth [7] intended to replace R12 in a hermetic vapor compression system and conducted experiments with R290 and R290/R600a mixtures. Regarding a composition of 50% propane by mass, the COP was improved and a similar saturation characteristic was scored. Based on those results, it is stated that the mixture can be used in an unmodified R12 system. Similar approaches for domestic refrigerators regarding propane and isobutane mixtures were conducted by Refs. [8] and [9]. Further references also with respect to HFC, HFC/HC and azeotropic mixtures can be found in the review of Mohanraj [3]. Many researchers also reported [4], [10], [11] that the heat transfer coefficients of zeotropic mixtures decrease. Summarizing, the reported experimental investigations show that the benefit of mixtures with respect to the COP is often only marginal, and therefore, contradicting the basic theoretical approach while the reason for the discrepancy remains unclear. However, if the experiments are reviewed, it is noted that it was not yet considered to optimize the targeted use of the mixture, meaning with heat sources with considerable change in temperature and also varying this temperature change.

In zeotropic fluid mixtures further complications may occur: because of different vapour and liquid flow rates, composition shifts can occur [12]. It is conceivable that besides the TG and thus decreasing exergy loss in the heat exchangers, other components (e.g. the compressor) or properties may be negatively influenced by the use of a zeotropic mixture. Up to now, experimental investigations with respect to the influence on single components with respect to the temperature change of the heat source are lacking.

Aiming to improve this situation, we investigated the influence of three different heat capacity flowrates of the secondary fluid within the evaporator on the complete cycle and on each component, for a mixture and for pure compounds, respectively. The change in heat capacity flowrate leads to better or worse matching of the temperature glide of the mixture and the temperature variation of the heat source; their influence is investigated. It is assumed that sometimes the reduction of exergy losses in the evaporator may be overcompensated by larger exergy losses in other parts. Isobutane/propene mixture (42:58) with a TG of 8.03 K is investigated as working fluid, together with investigations of the pure fluids isobutane and propene, all for equal boundary conditions. All experiments were carried out for an evaporator inlet temperature of 0°C and two compressor rotation speeds (1050 min⁻¹ / 2100 min⁻¹). The exergy losses of individual components, and performance factors for the whole cycle, like exergetic efficiencies and COPs, were determined and are compared.

2. Experiments

2.1 Experimental setup and measurement equipment

The experimental setup with the main components of the heat pump is schematically shown in Fig. 1; it contains a compressor, an expansion valve, a condenser, an evaporator, liquid tank reservoir and further auxiliary valves in order to be able to control the mass flow of the heat source and sink. It was already described previously [14], more details were given there. For later referencing, the states are numbered in Fig. 1.

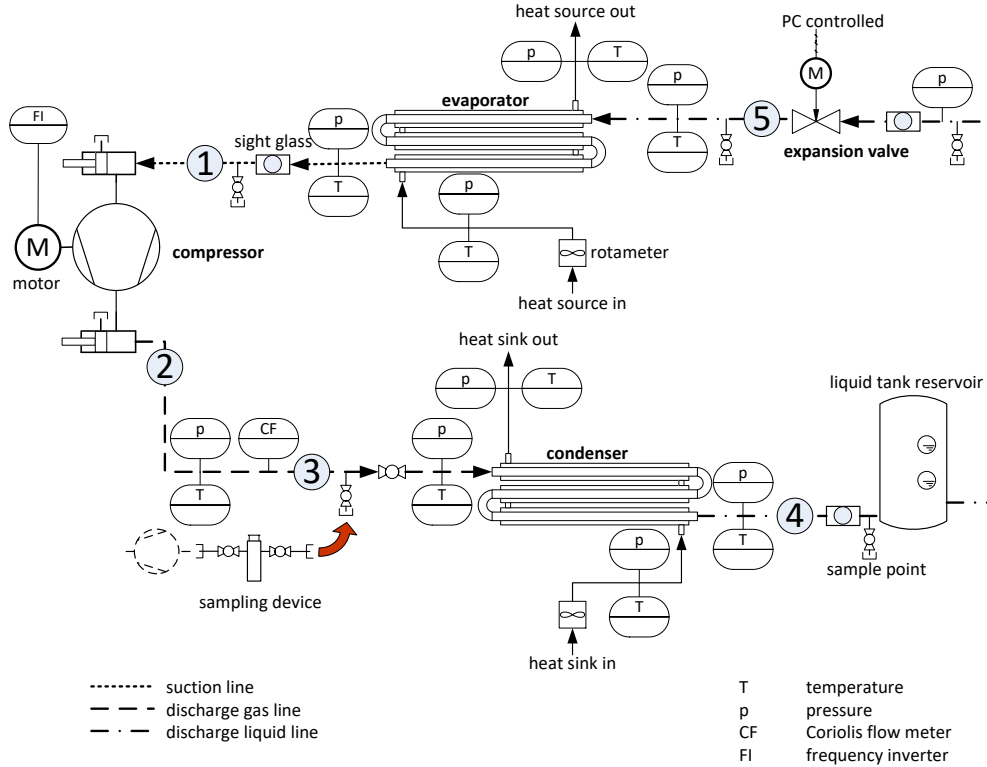
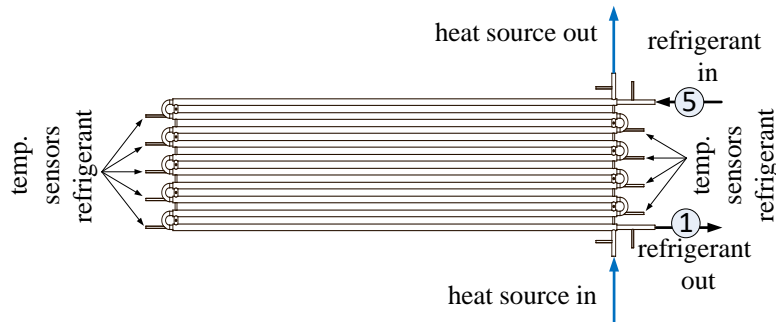


Fig. 1: Schematic flowchart of the experimental rig.

A semi-hermetic reciprocating compressor was used which was specially developed for hydrocarbons such as isobutane, propane and propene. It has two cylinders, a displacement volume of 5.4 m³/h and a maximum electrical power intake of 2.2 kW. Furthermore, the compressor is equipped with a frequency inverter whereby the rotation speed can continuously be varied and controlled between 1050 min⁻¹ and 2100 min⁻¹ while the electrical power consumption is monitored. The evaporator as well as the condenser are designed as double-pipe counter flow heat exchangers. According to Fig. 2, each heat exchanger consists of 10 straight sections with a length of 1.4 m connected by 180° return bends (elbows). The total heat transfer areas of the evaporator and condenser are 0.5 m² and 0.75 m², respectively. In both, the refrigerant always flows through the inner tube (evaporator: inner diameter $d_i = 10$ mm; wall thickness $d_w = 1$ mm, condenser: $d_i = 13$ mm; $d_w = 1.5$ mm), meanwhile the secondary heat transfer fluid (water) flows through the annulus ($d_i = 16$ mm for the evaporator, 19 mm for the condenser). The flow rate of water in each heat exchangers is regulated with a needle valve. To minimize heat losses, the heat exchangers, every sensor, as well as every connecting pipe are isolated with polyurethane foam of 20 mm thickness. At the inlets, outlets, and at every return bend (see Fig. 2) of the heat exchangers, the temperatures of the refrigerant and the secondary heat transfer fluid, are measured by resistance thermometers. In addition, pressures are recorded at the inlets and outlets. Sight glasses have been installed before and after the receiver tank and just before the compressor, in order to determine

visually the state of the refrigerant (liquid or vapour or saturated) and react accordingly when needed.

a



b

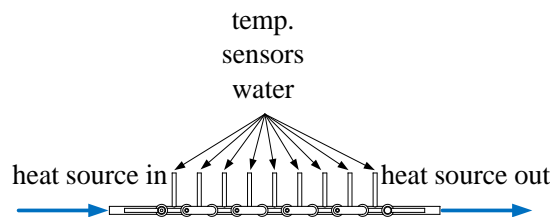


*Fig. 2: Schematic working plan of the heat exchanger **a**: top view and **b**: side view.*

Next to the sight glasses, sampling points are mounted in order to take specimens of the refrigerant. A gas chromatograph (GC) with a relative error of 2 % is used to determine the composition of the mixture. The refrigerant mass flow rate is quantified accurately by a Coriolis flow meter. At the inlet and outlet of the flow meter, temperature and pressure transducers are installed to characterize the flow meter and the compressor in detail. The mass flow rates of the secondary heat transfer fluid in the evaporator and condenser are recorded by turbine flow sensors (referred to in Fig. 1 as rotameter). A high precision needle valve which is controlled incrementally by a step motor is used here as the expansion valve. Changing the flow cross-section of the expansion valve allows the regulation of the pressure, and thus, the regulation of the evaporation temperature and degree of superheating. In order to perform experiments for different compressor rotation speeds, a liquid tank reservoir (7.5 liter) buffers excess refrigerant, because the refrigerant charge depends on the compressor rotation speed, and also, to damp fluctuations after changing the experimental conditions. The charge of the cycle strongly depends on the mean density of the fluid; the values for isobutane, propene and for the investigated mixture are 152 g, 730 g and 352 g, respectively.

The 42 resistance thermometers, 6 pressure sensors, 2 rotameters, and the Coriolis flowmeter, as well as the servo-motor of the expansion valve and the frequency inverter are all connected to a PC by a USB multifunction DAQ device. The software tool LabVIEW [13] is used for monitoring, recording and controlling the experiments; all values are recorded every second. Based on given tolerances from the manufacturers of the used measurement equipment, the statistical error is estimated from error propagation; the calculated relative error (1σ) of the COP_H is 2.21 %. To validate this value, selected experiments were reproduced and resulted in a maximum relative deviation of 2.5 %.

2.2 Investigated parameters

In the present work systematic experiments were carried out to analyse the relation between the exergy losses in the evaporator and the resulting influence on the entire process. The exergy losses in the evaporator are varied by the adaptation of the temperature differences between the working fluid and the heat source. The targeted utilization of the TG is achieved by matching the

temperature variation of the mixture and the temperature variation of the heat source; this was adjusted by varying the heat capacity flowrate (between 113.21 W/K and 509.38 W/K) of the secondary fluid water. The water inlet temperature of the evaporator and condenser are both constant at 17 °C and 25 °C, respectively. For all investigations, the outlet temperature of the heat sink is kept constant at 35 °C by varying the mass flow rate of the heat sink (between 1.4 kg min⁻¹ and 6.87 kg min⁻¹). The fixed heat sink temperature difference of 10 K is chosen due to typical floor heating applications. According to the second law, the irreversibility, and thus, the exergy loss, of a heat transfer process is directly related to the mean temperature difference between both fluids. For each compressor rotation speed and respective evaporator inlet temperatures of the working fluid, three different exergy loss scenarios are considered. For given conditions, the first case with negligible superheating represents the lowest exergy loss in the evaporator and thus, the best possible temperature matching between the working fluid and the heat source. In the third case, the highest exergy loss is applied for the evaporator (no temperature matching at all) while the second case is an intermediate case with a superheating of at least 6 K. To obtain comparable results for all investigated scenarios, the thermodynamic state at the inlet of the evaporator was controlled accurately. The fluctuation of the mass flow rate is lower than 1.2 %. After reaching steady state conditions, the data were recorded for 20 min, for averaging the values.

2.3 Data reduction

In order to analyse a vapour compression heat pump cycle thermodynamically, fluid properties like enthalpies and entropies as a function of the measured properties temperature and pressure are needed. Here, the REFPROP [13] database is used for all fluids. From the first law of thermodynamics the heat transfer rate from the source \dot{Q}_L and to the sink \dot{Q}_H are calculated:

$$\dot{Q}_{w_i} = \dot{m}_{w_i} \cdot (h_{w_i,out} - h_{w_i,in}). \quad (1)$$

The coefficient of performance for the heat pump is calculated using also the measured compressor electrical power intake:

$$\text{COP}_H = \frac{|\dot{Q}_{w_H}|}{P_{el}}. \quad (2)$$

The global compressor efficiency $\eta_{\text{compressor}}$, including the mechanical and the isentropic efficiencies, is derived by:

$$\eta_{\text{compressor}} = \frac{\dot{m}_{\text{Ref}} \cdot (h_{2,is} - h_1)}{P_{el}}. \quad (3)$$

Except the state at the evaporator inlet, all other states of the cycle are fully thermodynamically defined by the measured temperatures and pressures. The evaporator inlet state is saturated; thus for pure fluids p and T are not sufficient to fix the state. Thus the energy balance is used to calculate the enthalpy, assuming an adiabatic evaporator:

$$h_5 = h_1 - \frac{\dot{m}_{w_L}}{\dot{m}_{\text{Ref}}} \cdot (h_{w_L,in} - h_{w_L,out}). \quad (4)$$

Due to the fact that the evaporator is insulated and furthermore, the difference between the heat source and the surrounding is only 5 K in average, the assumption of an adiabatic evaporator is justified. For fluid mixture with known composition (which is verified experimentally by GC), a state in the two phase region is uniquely defined by temperature and pressure.

Besides the energetic analysis, exergies are analyzed. The exergy flow rate of each state is calculated from:

$$\dot{E}_i = \dot{m}_i \cdot ((h_i - h_0) - T_0 \cdot (s_i - s_0)). \quad (5)$$

State 0 indicates the surrounding conditions. The exergy loss of a component, “i” is calculated from equation (6) as the difference between the inlet and the outlet exergy flow rates $\dot{E}_{i_{in}}$ and $\dot{E}_{i_{out}}$, and the electrical power P_{el}

$$\dot{E}_{li} = \sum \dot{E}_{i_{in}} - \sum \dot{E}_{i_{out}} + P_{el} \quad (6)$$

The second law efficiency is defined as follow:

$$\eta_{\text{exergy}} = 1 - \frac{\sum \dot{E}_{li}}{P_{el}} \quad (7)$$

It should be noted, that the exergy needed to provide the water mass flow rates in the heat source and the heat sink were not considered here.

The temperature glide TG, used to characterize a non-isothermal phase change, is defined as the difference between the dew and bubble point temperatures at constant pressure:

$$TG = T_{\text{dew}} - T_{\text{bubble}} \quad (8)$$

The TG is completely utilized in the condenser, but in the evaporator, the pressure loss and the saturated state at the inlet, after passing the throttle, reduce the usable TG and is approximated by:

$$TG_{\text{ev}} = T_{\text{vap}}(p_{\text{ev}_{out}}, q = 1) - T_{\text{ev}_{in}} \quad (9)$$

3. Results and discussion

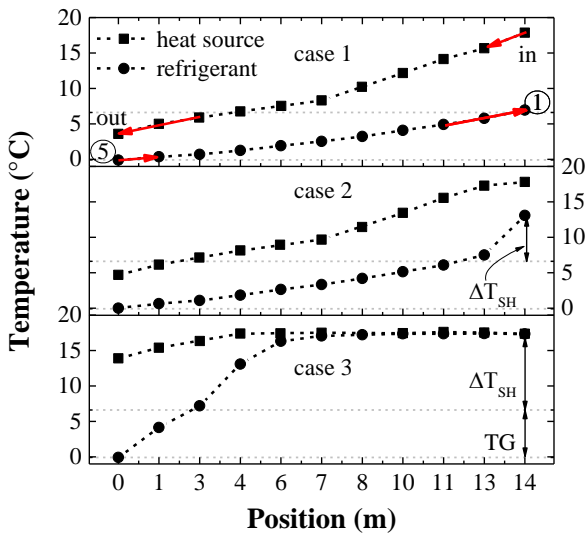


Fig. 3: Temperature profile of the refrigerant and the heat source in the evaporator as a function of evaporator length for $T_L = 0 \text{ }^\circ\text{C}$, $n = 1050 \text{ min}^{-1}$ and three different heat capacity flows.

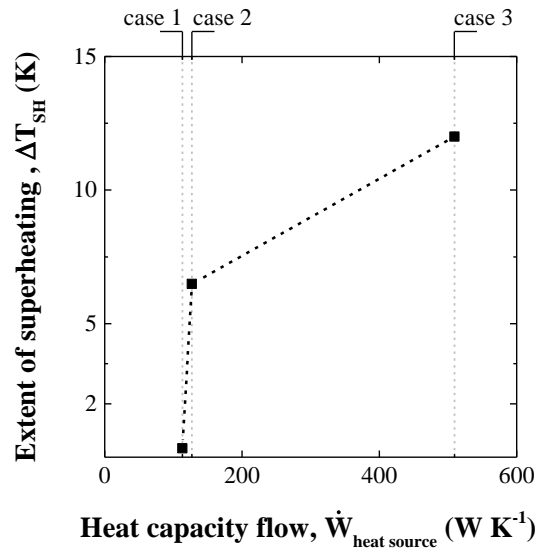


Fig. 4: Attained superheating of the refrigerant as a function of heat capacity flow for $T_L = 0 \text{ }^\circ\text{C}$; $n = 1050 \text{ min}^{-1}$.

Three different evaporator exergy loss scenarios are compared:

- Case 1 in Fig. 3: lowest exergy loss, lowest heat source capacity flow rate of 113.2 W / K , negligible superheating
- Case 2 in Fig. 3: medium exergy loss and a superheating of 6 K , medium heat source capacity flow rate of 126.9 W / K

- Case 3 in Fig. 3: highest exergy loss, highest heat source capacity flow rate of 509.4 W / K

The measured temperature profiles of the heat source and the mixture along the evaporator position are illustrated in Fig. 3 for the three investigated evaporator exergy loss scenarios (cases), all at a compressor rotation speed of $n = 1050 \text{ min}^{-1}$. For the sake of clarity, the attained superheating of the refrigerant as a function of the heat capacity flow for the three cases at $n = 1050 \text{ min}^{-1}$ is again shown in Fig. 4.

Since both, the state of the mixture at the inlet of the evaporator, as well as the pressure drop in the evaporator, remain approximately constant for all experiments, the temperature glide of the mixture remains constant as well. Due to equation (9), the actually usable TG of the mixture within the evaporator is 6.18 K as illustrated in Fig. 3 by the grey dashed lines. With decreasing heat source capacity flowrate (from case 3 to case 1), the superheating temperature of the refrigerant decreases on one hand (Fig. 4) and the temperature matching between the refrigerant and the heat source is improved on the other hand, as can be seen in Fig. 3. This relation is easily explained: Reaching the dew temperature, (crossing point of the refrigerant temperature profile with the grey dashed line in Fig. 3) the evaporation is completed and the superheating of the refrigerant begins. With decreasing heat source capacity flow rate (from case 3 to case 1), the mean temperature difference between the refrigerant and the heat source decreases as well. Thus, a larger part of the heat transfer area is needed to evaporate the refrigerant. Therefore, the evaporation and the temperature glide take place throughout the whole evaporator and the desired temperature matching between the refrigerant and the heat source is achieved (Fig. 3, case 1 and case 2). The variation of the capacity flowrate leads to changes in the amount of superheating of the refrigerant, and thus, the compressor inlet conditions change. This coupled interaction between the different components affects the entire process as can be seen in Fig. 5, although it was intended to vary only a single heat capacity flowrate.

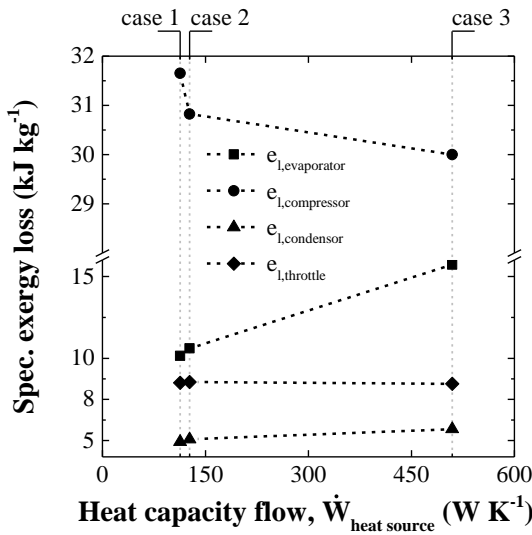


Fig. 5: Specific exergy loss of each component as a function of the heat source capacity flow for $n = 1050 \text{ min}^{-1}$.

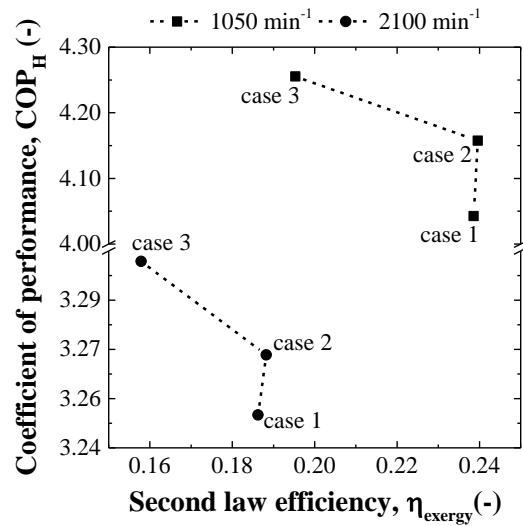


Fig. 6: Coefficient of performance as a function of the exergetic efficiency for investigated scenarios; $n = 1050 \text{ min}^{-1}$ and $n = 2100 \text{ min}^{-1}$.

Figure 5 shows the specific exergy loss of the components as a function of the heat source capacity flowrate for $n = 1050 \text{ min}^{-1}$ with an interrupted ordinate. First of all, it can be observed that the specific exergy loss in the evaporator decreases with decreasing heat capacity flowrate (from case 3 to case 1). In agreement with the targeted utilization of the TG, the thermodynamic mean

temperature difference between the refrigerant and the heat source increases and thus the specific exergy loss also increases with the heat capacity flowrate. Operating points with the lowest exergy losses also have the lowest amount of superheating (compare Fig. 5 and Fig. 4). Independent of the heat source capacity flowrate, the highest specific exergy loss is always found in the compressor, followed by the evaporator, the throttle and the condenser. By means of reducing the heat source capacity flow rate, the specific exergy losses of the evaporator and condenser are decreased by 35.29 % and 13.71 %, respectively, while the exergy loss of the compressor increases by 6.55 %. The exergy loss of the throttle is independent of the heat source capacity flow rate due to a constant pressure difference between evaporator and condenser. Also the reduced exergy loss in the condenser from case 3 to case 1 is easy to explain. Due to a reduced compressor inlet temperature, the compressor outlet temperature also decreases. For constant heat source inlet and outlet temperatures, a reduction of the compressor outlet temperature leads to a reduced mean temperature difference and thus to a reduction of the exergy loss within the condenser. The exergy loss of the entire process is reduced by 7.17 %, which in turn also leads to an improved exergetic efficiency as shown.

The coefficient of performance as a function of the exergetic efficiency regarding the investigated scenarios, for $n = 1050 \text{ min}^{-1}$ and $n = 2100 \text{ min}^{-1}$ is shown in Fig. 6, again, with an interrupted ordinate. For a compressor rotation speed of $n = 1050 \text{ min}^{-1}$, the COP_H decreases by 4.2 % (from case 3 to case 1) while the second law efficiency increases by 18.15 % primarily due to a reduction of the evaporator exergy loss, leading to lower output temperatures of the water, which increases the outflowing exergy flow rate. Regarding the compressor rotation speed of 2100 min^{-1} , the COP_H decreases by 1.6 % and the second law efficiency increases by 14.78 %. Of course, the change of the COP_H is very small and near to the experimental uncertainty, especially for $n = 2100 \text{ min}^{-1}$, but for all investigated evaporator inlet temperatures and compressor rotation speeds, the same trend can always be observed. Here, the exergetic optimization of the process is not directly related to the COP of the process, because the COP for a heat pump does not consider the exergy gain in the low temperature fluid.

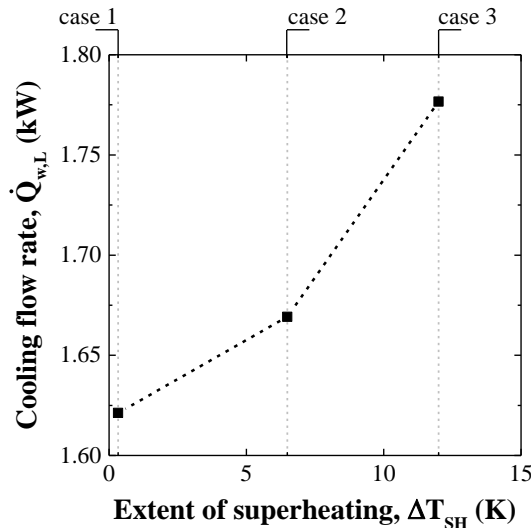


Fig. 7: Evaporator cooling flow rate as a function of superheating for $n = 1050 \text{ min}^{-1}$.

Figure 7 shows the dependence of the source heat flowrate on the superheating at $n = 1050 \text{ min}^{-1}$. With an equal refrigerant state (Fig. 1 state 5) at in the inlet of the evaporator and similar mass flow rate of the refrigerant for all scenarios, the transferred energy directly depends on the superheating and increases (by 8.5 %) with higher superheating. This also influences the specific exergy loss as well as the global efficiency of the compressor as shown in Fig. 8; the direct relation between superheating and compressor efficiency is shown in Fig. 9. The compressor efficiency decreases

with decreasing superheating from case 3 to case 1 by 5.15 %, while its exergy loss increases by 6.55 %. This raises the question, where this strong difference may originate. After considering several possible reasons, we think that the most probable explanation may be the temperature dependent solubility of the working fluid in the lubricant oil, similar results were reported earlier [16]. The primary use of a lubricant in a compressor is the reduction of the friction between piston and cylinder, thus minimizing mechanical losses. Additionally, the lubricant has also a sealing function between the piston and the cylinder. Both fluids used here, R290 and R600a, are soluble in polyalphaolefin oils [15]. The lubricant fluid cannot be considered as a pure fluid, rather as a refrigerant-lubricant mixture whose lubricating properties vary significantly from those of a pure oil. Solubility depends on temperature and pressure and thus on the superheating temperature of the entering working fluid and on the evaporation/condensation pressure. The latter are constant here, thus superheating must be crucial. With decreasing superheating at the inlet of the compressor, the solubility of refrigerant/oil increases; thus, lubrication and sealing properties of the oil-refrigerant mixture probably worsen and finally, the efficiency of the compressor decreases. In Ref. [16] the influence of the extent of superheating on the global efficiency was investigated for a semi-hermetic reciprocating compressor (manufacturer: Bitzer) specially designed to operate with R290. The main result was the strong negative influence on the lubrication and sealing properties of the oil caused by increased propane solubility due to decreased superheating in the suction line and thus decreased compressor efficiency. Considering the fact that the compressor manufacturer suggests a minimum superheating of 20 K in order to operate the compressor in a good operating point, this is rather counterproductive for a targeted utilization of the TG.

To summarize, first of all a very good temperature match between the zeotropic mixture and the heat source induced by the targeted utilization of the zeotropic mixture TG results in a minimized exergy loss in the evaporator and leads also to a high second law efficiency. The utilization of the TG in the evaporator, in turn, results in a lower heat flow rate, and thus, in a reduced superheating. This decreases the compressor efficiency and finally leads to a decreased COP of the entire cycle.

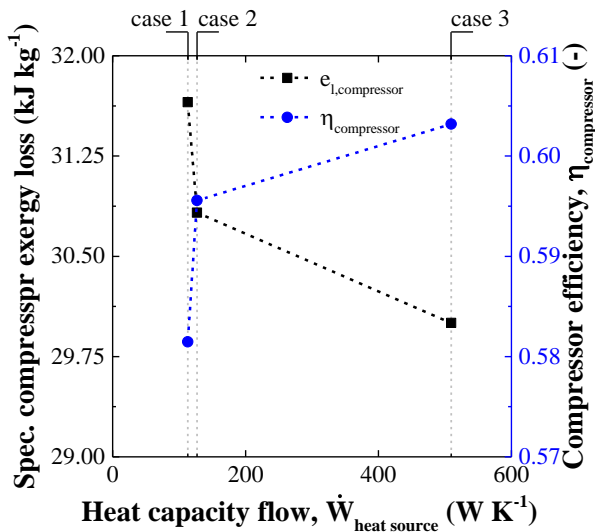


Fig. 8: Specific exergy loss and the global compressor efficiency of the compressor as a function of the heat source capacity flow for $n = 1050 \text{ min}^{-1}$.

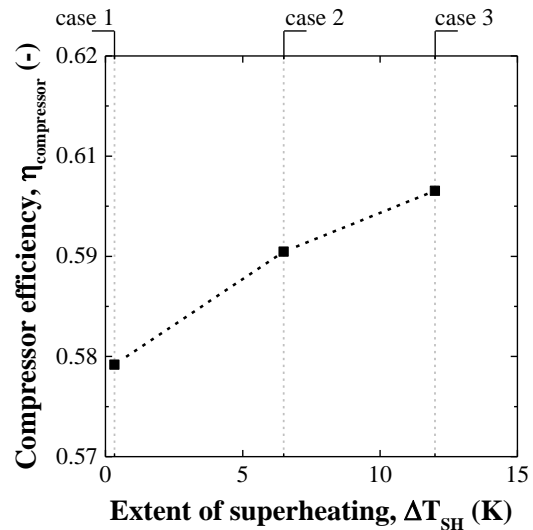


Fig. 9: Compressor efficiency as a function of the extent of superheating for $n = 1050 \text{ min}^{-1}$.

Besides the mixture, also the pure fluids isobutane and propene were investigated for the case of lowest (case 1) and highest exergy loss (case 3) within the evaporator for comparison. The exergy losses of the different components are shown as a function of propene mole fraction for case 1 in Fig. 10 and case 3 in Fig. 11, both for $n = 1050 \text{ min}^{-1}$. Starting from pure isobutane, all exergy

curves are lower for the mixture and increase again for pure propene. As expected, for both heat exchangers, the exergy loss is smaller for the mixture, but the benefit of the mixture is small. Comparing the two cases, the difference is most obvious for the evaporator, as expected, while the exergy losses are throughout dominated of the compressor and are strongly decreasing from isobutane towards propene.

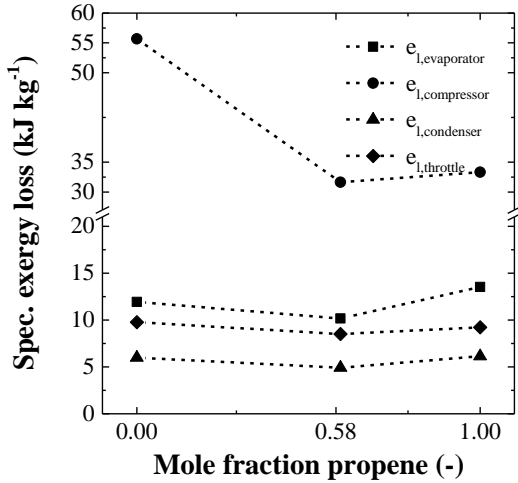


Fig. 10: Specific exergy loss of each component as a function of the propene mole fraction for $n = 1050 \text{ min}^{-1}$ with the aim of minimizing the exergy loss (case 1).

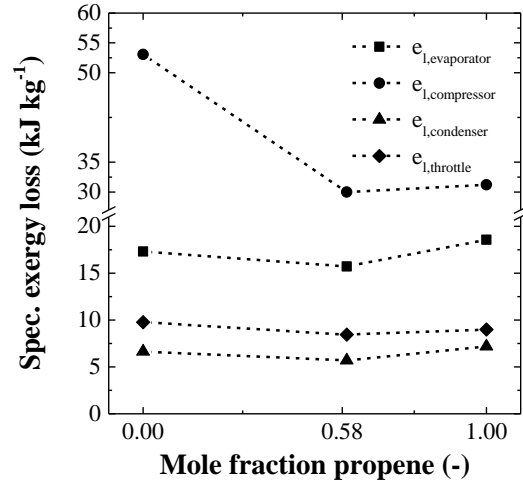


Fig. 11: Specific exergy loss of each component as a function of the propene mole fraction for $n = 1050 \text{ min}^{-1}$ without the approach to minimize the exergy loss (case 3).

From case 3 to case 1, the compressor exergy loss for isobutane and propene increases by 4.91 % and 6.7 %, respectively, due to decreased superheating. So it may turn out, that in view of the total system performance, it is more important to investigate lubricants with low solubility for hydrocarbons than investigating the influence of mixtures on heat exchanger losses.

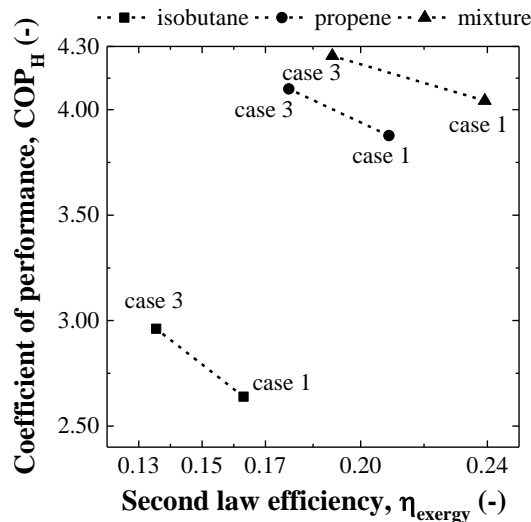


Fig. 12: Coefficient of performance as a function of the second law efficiency for $n = 1050 \text{ min}^{-1}$ for isobutane, propene and the mixture with respect to lowest and highest exergy loss scenario.

The coefficient of performance as a function of the second law efficiency is shown in Fig. 12 for isobutane, propene and the zeotropic mixture. They are not going in line, because the exergy in the cold water (not considered in the COP_H) is high for case 1, while the compressor power is also large in this case, due to low superheating. However, for all cases, the mixture always reaches the highest coefficient of performance as well as highest second law efficiency, but the effect is moderate compared to propene. Thus, every theoretical assumption has to be considered in the light of technical conditions and constraints which may considerably lower the predicted advantages of a certain process, as the use of zeotropic mixtures.

4. Conclusion

Three working fluids for a vapor compression heat pump, isobutane, propene and a zeotropic mixture of isobutane/propene (42:58), were investigated experimentally as a function of heat capacity flow in the evaporator. A general improvement with respect to the coefficient of performance is observed using a zeotropic mixture as a working fluid, but the achieved improvements are far lower than the predicted ones from simple thermodynamic calculations (with constant isentropic efficiency for the compressor).

Zeotropic mixtures should improve the coefficient of the performance due to a reduction of the exergy losses in the heat exchangers due to the TG. This was investigated for different heat capacity flowrates and thus different temperature changes of the secondary fluid. This directly varies the usage of the temperature glide.

Although it turns out, that the exergy losses in the evaporator are reduced for better matching situations, this is nearly compensated due to the reduced superheating of the working fluid entering the compressor, which in turn leads to reduced efficiencies of the compressor. It is assumed, in accordance with the literature, that differences in the superheating of the fluid lead to different solubility in the lubricant oil of the compressor and thus to more friction, and probably also to a changed sealing effect between the cylinder and the piston. Since the exergy losses in this system are dominated by the exergy losses of the compressor, the improvement of the total system remains small. The investigations show the importance of the entire cycle performance which should be kept in mind while improving individual components, as e.g. the heat transfer characteristics in the evaporator. It may turn out that it may be quite important to find lubricants with lower solubility of the working fluids for full utilization of the potential of zeotropic mixtures in thermodynamic cycles.

5. Acknowledgment

We thank KROHNE Germany for provision of some technical measuring equipment.

Nomenclature

COP_H	coefficient of performance of a heat pump
\dot{E}	exergy flow rate of each state, kW
$e_l = \frac{\dot{E}_l}{\dot{m}_{Ref}}$	specific exergy loss of each component, $\text{kJ} \cdot \text{kg}^{-1}$
\dot{E}_l	exergy loss flow rate, kW
h	specific enthalpy, kJ kg^{-1}
\dot{m}	mass flow rate, kg s^{-1}
n	rotation speed of the compressor, min^{-1}
P_{el}	electrical power intake of the compressor, kW
p	pressure, bar
\dot{Q}	heat flow, kW
s	specific entropy, $\text{kJ kg}^{-1} \text{K}^{-1}$

T	temperature, °C
TG	temperature glide, K

Greek symbols

$\eta_{\text{compressor}}$	global efficiency of the compressor
σ	relative error, %

Subscripts

bubble	bubble point
dew	dew point
ev	evaporator
H	at high level (e.g. temperature, enthalpy, mass flow rate, heat flow rate in condenser) /heat pump
i	component
in/out	inlet/outlet
is	isentropic
L	at low level (e.g. temperature, enthalpy, mass flow rate, heat flow rate in evaporator)
Ref	working fluid (refrigerant)
SH	superheating, [K]
vap	vapour
w	secondary heat transfer fluid (water)
0	fluid properties/conditions at 20 °C and 1.01 bar

Acronyms

CFCs	chlorofluorocarbons
COP	coefficient of performance
DAQ	data acquisition
GC	gas chromatograph
HC	hydrocarbon
HCFC	hydrochlorofluorocarbon
HFC	hydrofluorocarbon
ORC	organic rankine cycle
TG	temperature glide

References

- [1] Regulation (EU) No 517/2014 of the European parliament and of the council of 16 April 2014 on fluorinated greenhouse gases and repealing Regulation, (EC) No 842/2006; Official Journal of the European Union 2014 (L 150/195).
- [2] Ahamed J.U, Saidur R., Masjuki H.H A review on exergy analysis of vapor compression refrigeration system. Renewable and Sustainable Energy Reviews 2011; 15 (3):1593–600.
- [3] Mohanraj M., Muraleedharan C., Jayaraj S. A review on recent developments in new refrigerant mixtures for vapour compression-based refrigeration, air-conditioning and heat pump units. Int. J. Energy Res. 2011; 35 (8):647–69.
- [4] Chang Y., Kim M., Ro S. Performance and heat transfer characteristics of hydrocarbon refrigerants in a heat pump system. International Journal of Refrigeration 2000; 23 (3):232–42.
- [5] Park K.-J., Jung D. Performance of heat pumps charged with R170/R290 mixture. Applied Energy 2009; 86 (12):2598–603.

- [6] Park K.-J., Jung D. Thermodynamic performance of HCFC22 alternative refrigerants for residential air-conditioning applications. *Energy and Buildings* 2007; 39 (6):675–80.
- [7] Richardson R.N, Butterworth J.S The performance of propane/isobutane mixtures in a vapour-compression refrigeration system. *International Journal of Refrigeration* 1995; 18 (1):58–62.
- [8] Jung D., Kim C.-B., Song K., Park B. Testing of propane/isobutane mixture in domestic refrigerators. *International Journal of Refrigeration* 2000; 23 (7):517–27.
- [9] Kuijpers L., Wit J. de, Janssen M. Possibilities for the replacement of CFC 12 in domestic equipment. *International Journal of Refrigeration* 1988; 11 (4):284–91.
- [10] Sun Z., Gong M., Li Z., Wu J. Nucleate pool boiling heat transfer coefficients of pure HFC134a, HC290, HC600a and their binary and ternary mixtures. *International Journal of Heat and Mass Transfer* 2007; 50 (1-2):94–104.
- [11] Wen M.-Y., Ho C.-Y., Hsieh J.-M. Condensation heat transfer and pressure drop characteristics of R-290 (propane), R-600 (butane), and a mixture of R-290/R-600 in the serpentine small-tube bank. *Applied Thermal Engineering* 2006; 26 (16):2045–53.
- [12] Rajapaksha L. Influence of special attributes of zeotropic refrigerant mixtures on design and operation of vapour compression refrigeration and heat pump systems. *Energy Conversion and Management* 2007; 48 (2):539–45.
- [13] LabVIEW Professional Development System: National Instruments; 2013.
- [14] Venzik V., Roskosch D., Atakan A. Propene/isobutane mixtures in heat pumps: an experimental investigation. *International Journal of Refrigeration* 2017.
- [15] Fuchs Schmierstoffe GmbH product information; RENISO SYNTH 68, PAO refrigeration machine oil; 03.15.
- [16] Da Riva E., Del Col D. Performance of a semi-hermetic reciprocating compressor with propane and mineral oil. *International Journal of Refrigeration* 2011;34(3):752–63.

Temperature glide matching in a zeotropic mixture heat pump

Venzik, Valerius; Atakan, Burak

This text is provided by DuEPublico, the central repository of the University Duisburg-Essen.

This version of the e-publication may differ from a potential published print or online version.

DOI: <https://doi.org/10.17185/duepublico/48403>

URN: <urn:nbn:de:hbz:464-20190404-101402-7>

Link: <https://duepublico.uni-duisburg-essen.de:443/servlets/DocumentServlet?id=48403>

License:

As long as not stated otherwise within the content, all rights are reserved by the authors / publishers of the work. Usage only with permission, except applicable rules of german copyright law.

Source: Proc. ECOS 2017 - 30TH Int. Conf. Effic. COST, Optim. Simul. Environ. IMPACT ENERGY Syst., San Diego, California, USA: 2017